Supplementary Materials

Preparation of Non-Toxic Fluorescent Peptide-Coated Silica/PEG Nanoparticles from Peptide-Block Copolymer Conjugates

Federica Santino [1,#], Pasquale Stavole [1,#], Tingting He [1], Silvia Pieraccini [1], Mayra Paolillo [2], Luca Prodi [1], Enrico Rampazzo [1,*], and Luca Gentilucci [1,*]

[1] Department of Chemistry "G. Ciamician", University of Bologna, via Selmi 2, 40126-Bologna Italy
[2] Department of Drugs Sciences, University of Pavia, 27100 Pavia, Italy
* L.G. E-mail: luca.gentilucci@unibo.it; Tel.: +39 0512099570; Fax: 39 0512099456;
web: https://site.unibo.it/mimepept/en
E.R. E-mail: enrico.rampazzo@unibo.it; Tel.: +39 0512099596

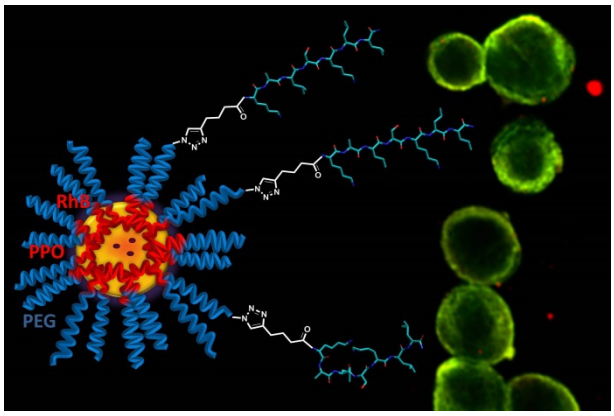

Contents

Figure S1-S3. RP HPLC and ESI MS of the peptides pS2
Figure S4. CD spectra of peptide^{+2} pS3
Figure S5-S6. ^{1}H-NMR of PF127 derivatives pS4
Figure S7. FT-IR spectra of PF127 derivatives pS5
Figure S8. ^{1}H-NMR of polymer-(peptide^{2+})$_2$, details pS5
Figure S9-S15. DLS, Zeta Potential, TEM analyses of NPs-peptides pS6

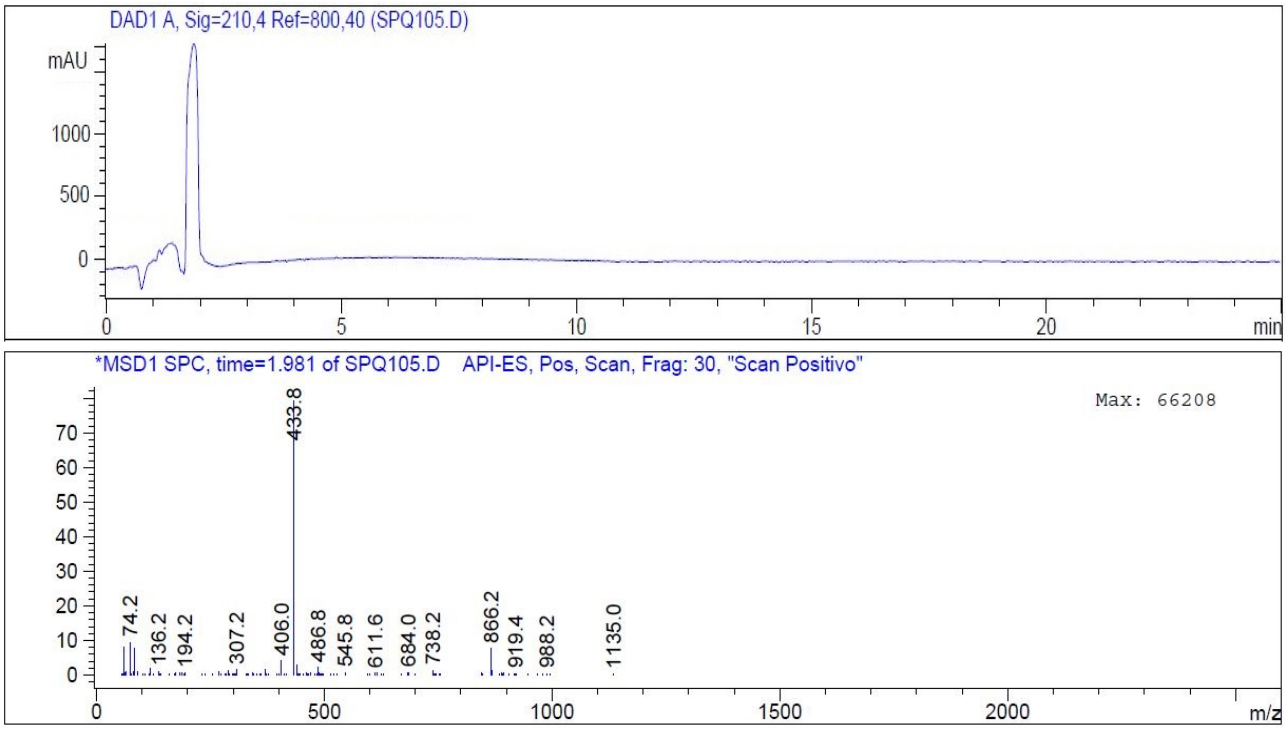

Figure S1. RP HPLC and ESI MS of peptide^{2+}.

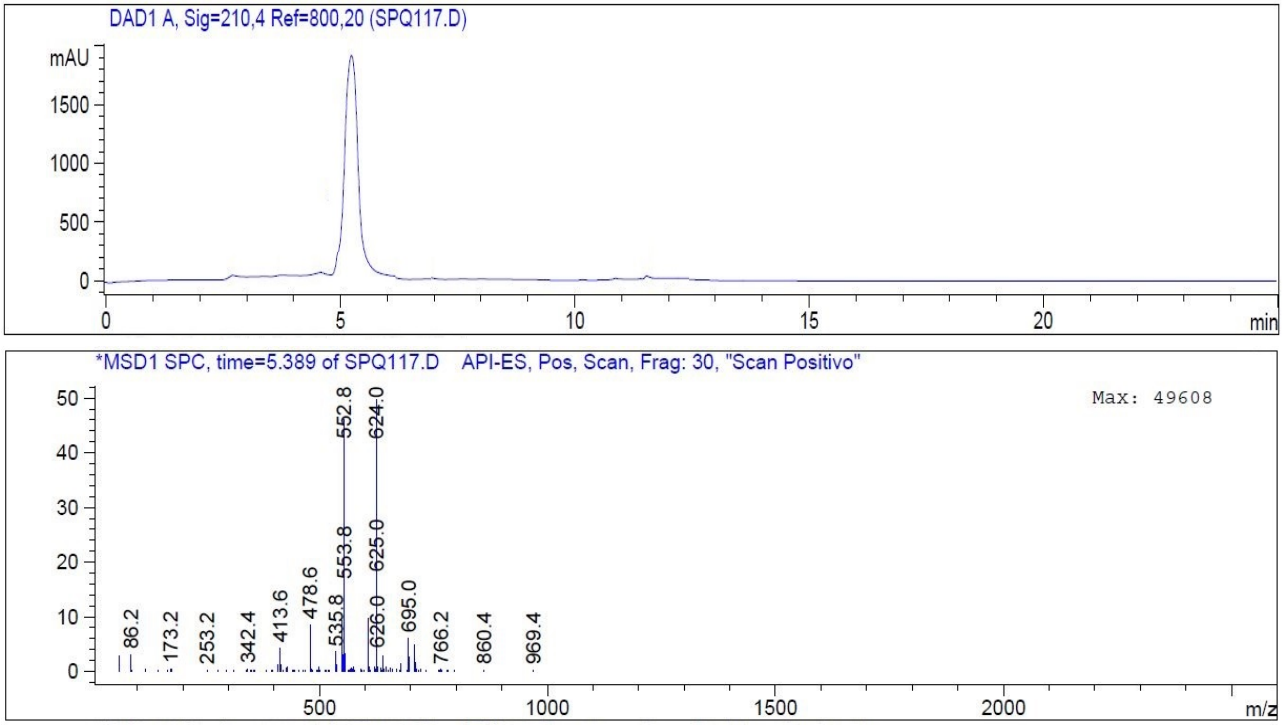

Figure S2. RP HPLC and ESI MS of peptide^{0}.

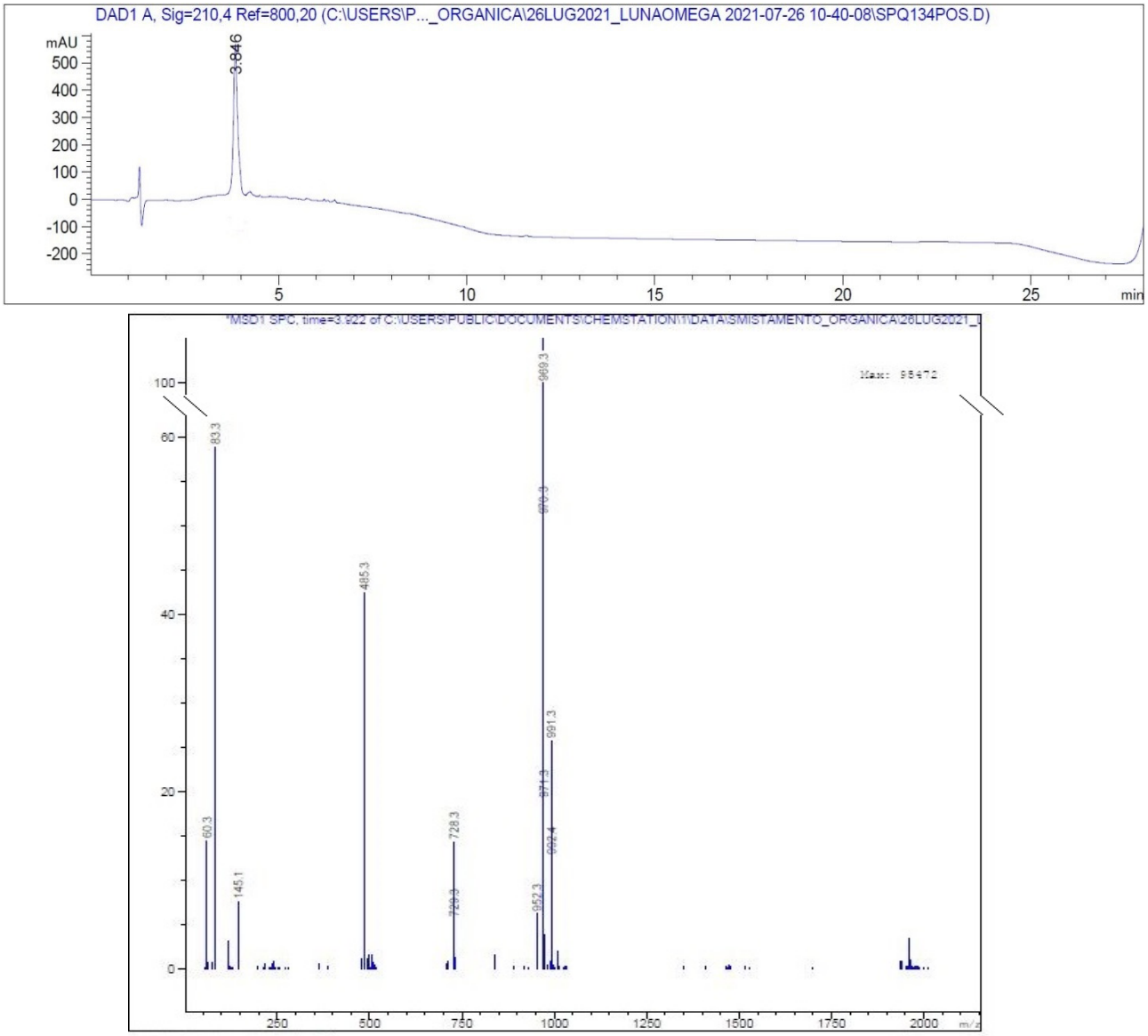

Figure S3. RP HPLC and ESI MS of peptide^{2-}.

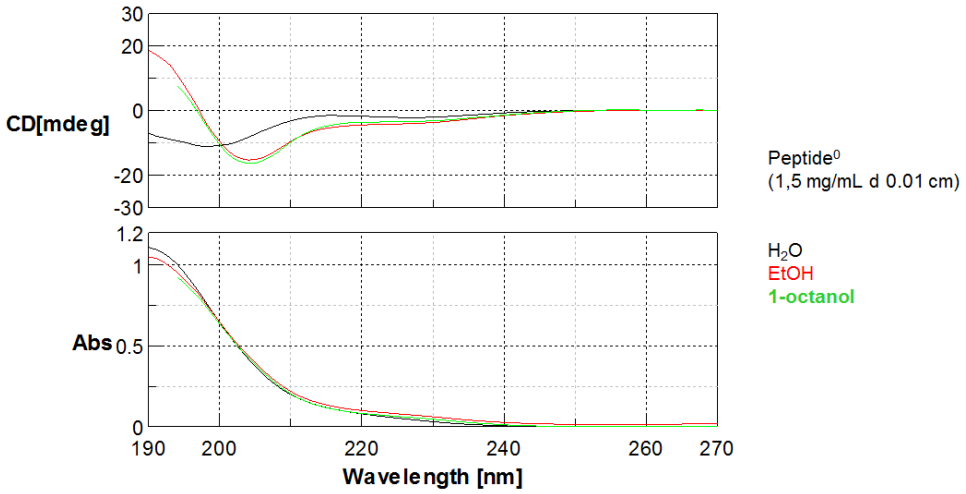

Figure S4. Circular dichroism spectra of peptide^{2+} (1.5 mg/mL d 0.01cm) in H2O (black), EtOH (red), EtOH/1-octanol 1:1 (green), EtOH/1-octanol 1:2 (blue)

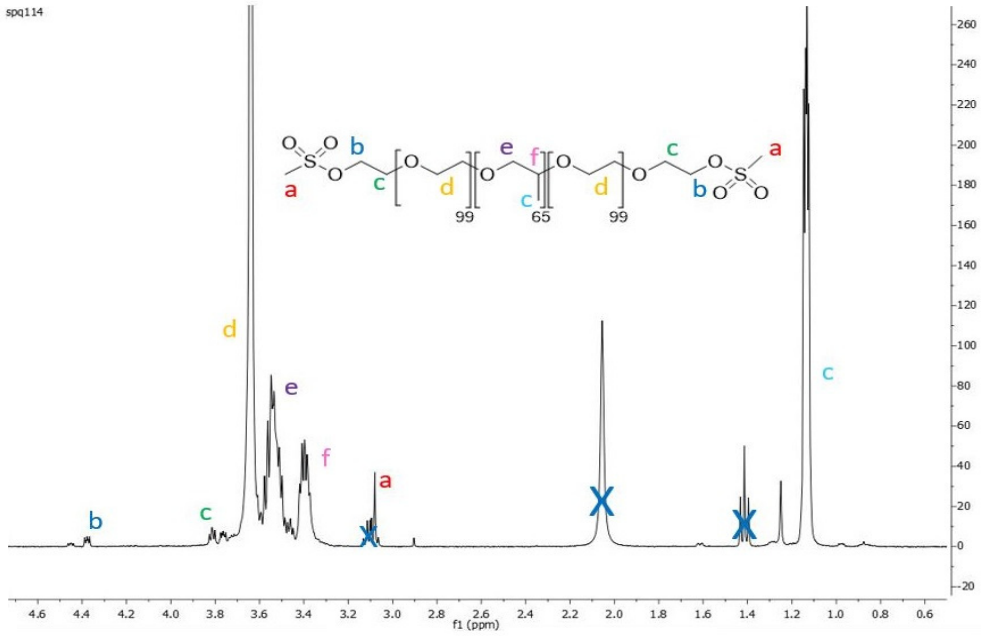

Figure S5. ^{1}H-NMR of dimesylated PF127, 400 MHz in $CDCl_3$.

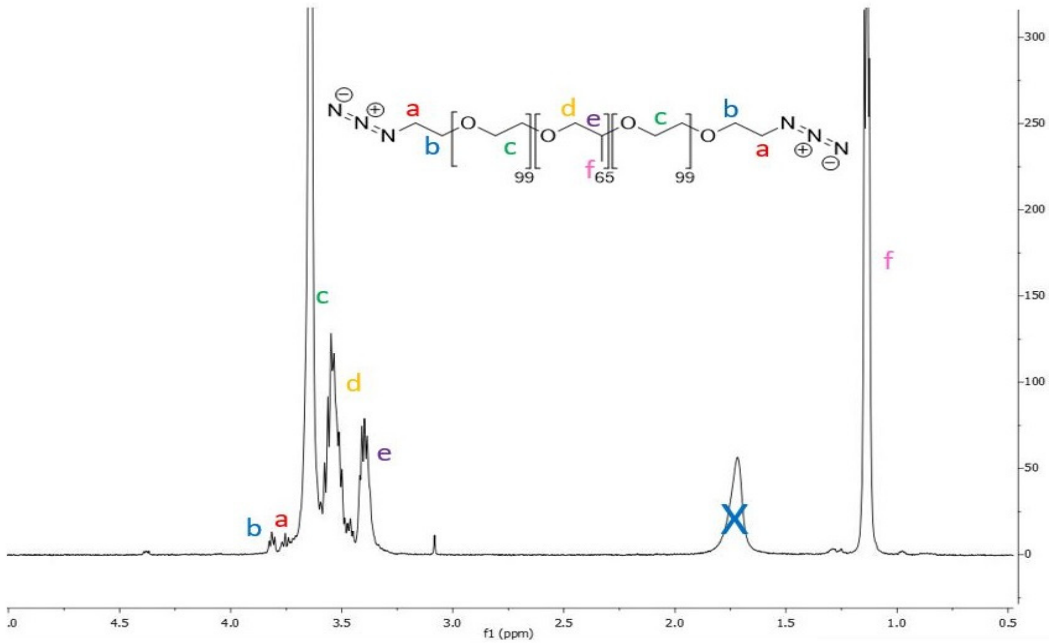

Figure S6. ^{1}H-NMR of the diazide derivative of PF127, 400 MHz in $CDCl_3$.

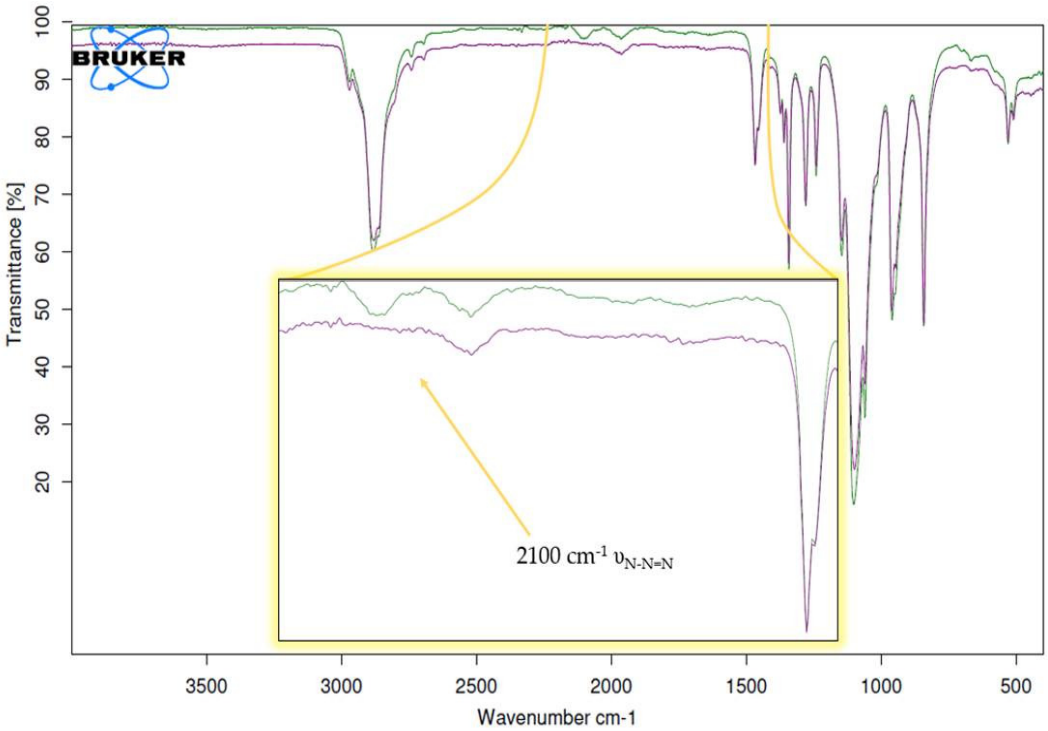

Figure S7. Superimposed FT-IR spectra of diazide derivative of PF127 (green) and PF127 (purple), with magnification in the area of interest around 2100 cm^{-1}.

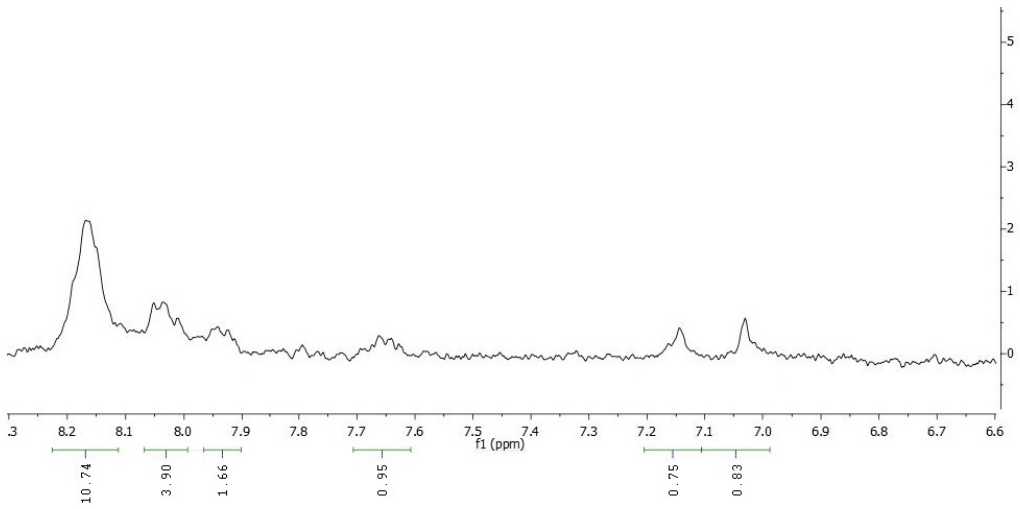

Figure S8. ^{1}H-NMR spectra of the amide region of polymer-(peptide^{2+})$_2$ with integrals, 400MHz, DMSO-d6; the integral of the reference peak of PPO methyls at 0.8 ÷ 1.1 ppm was set at 195 protons.

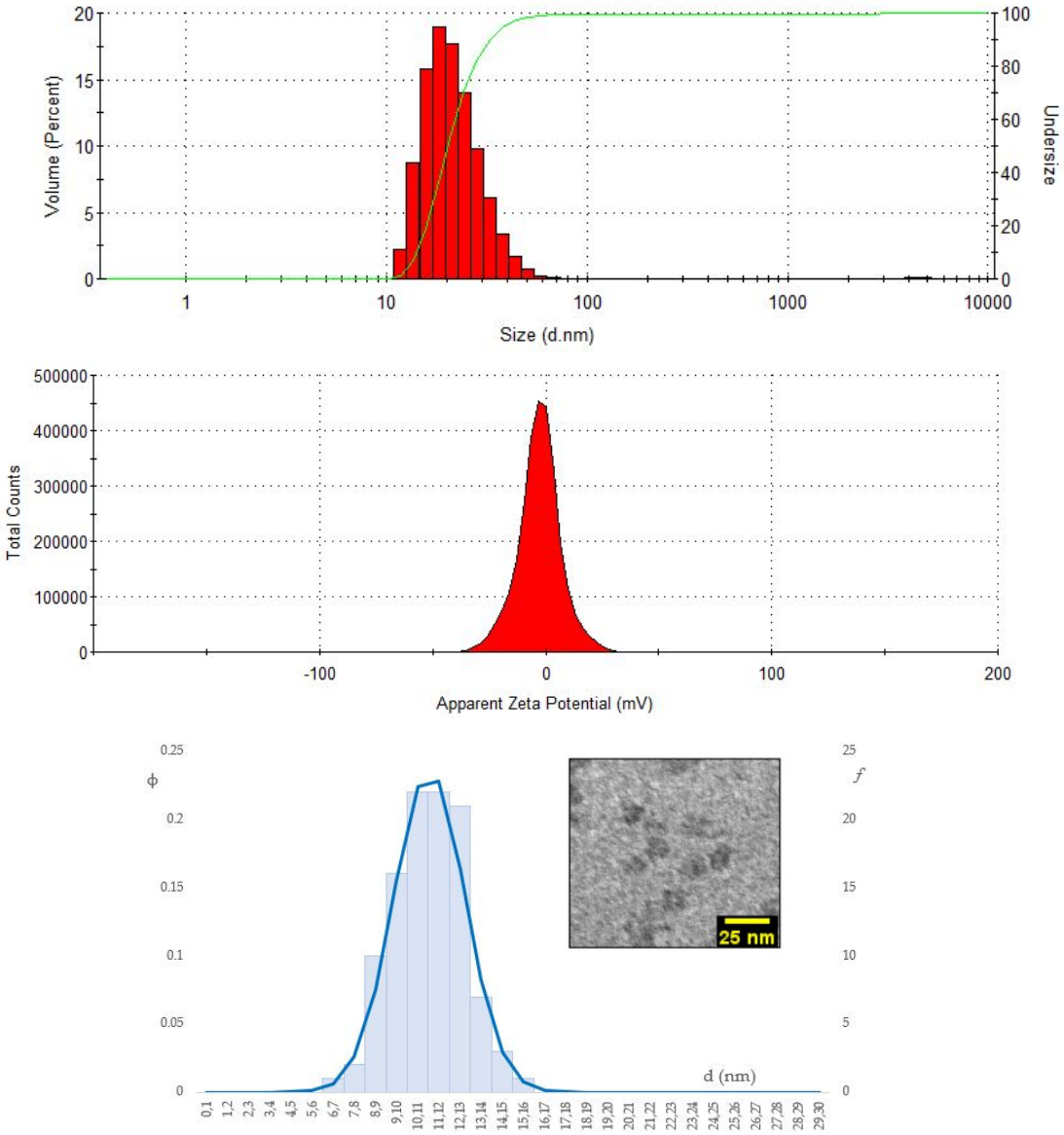

Figure S9. Top, DLS hydrodynamic size distribution by volume of NPs-10%peptide^{2+}; middle, Zeta Potential distribution of NPs-10%peptide^{2+}; bottom, TEM size distribution with representative image of NPs-10%peptide^{2+} (scale bar 25 nm).

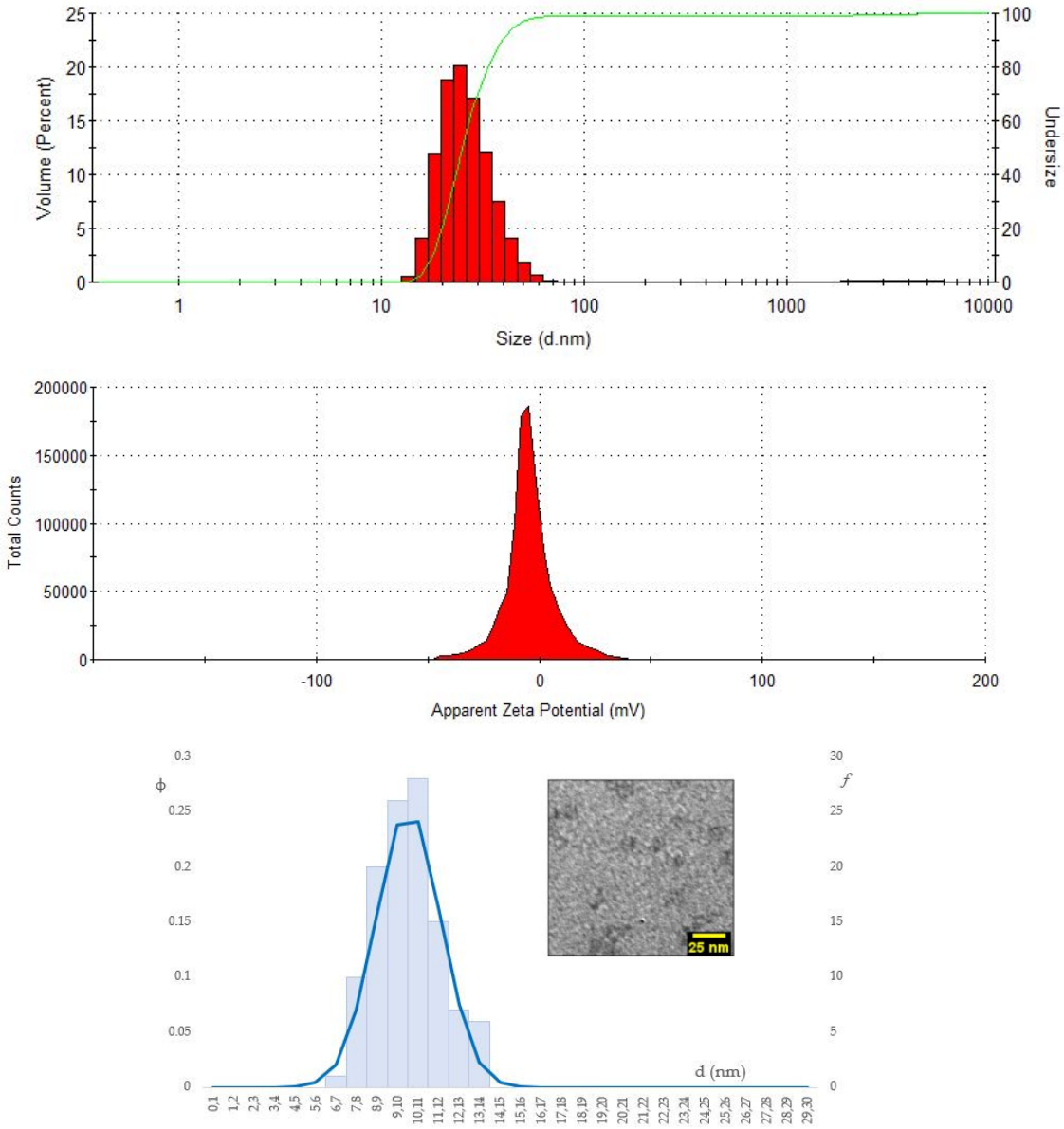

Figure S10. Top, DLS hydrodynamic size distribution by volume of NPs-20%peptide^{2+}; middle, Zeta Potential distribution of NPs-20%peptide^{2+}; bottom, TEM size distribution with representative image of NPs-20%peptide^{2+} (scale bar 25 nm).

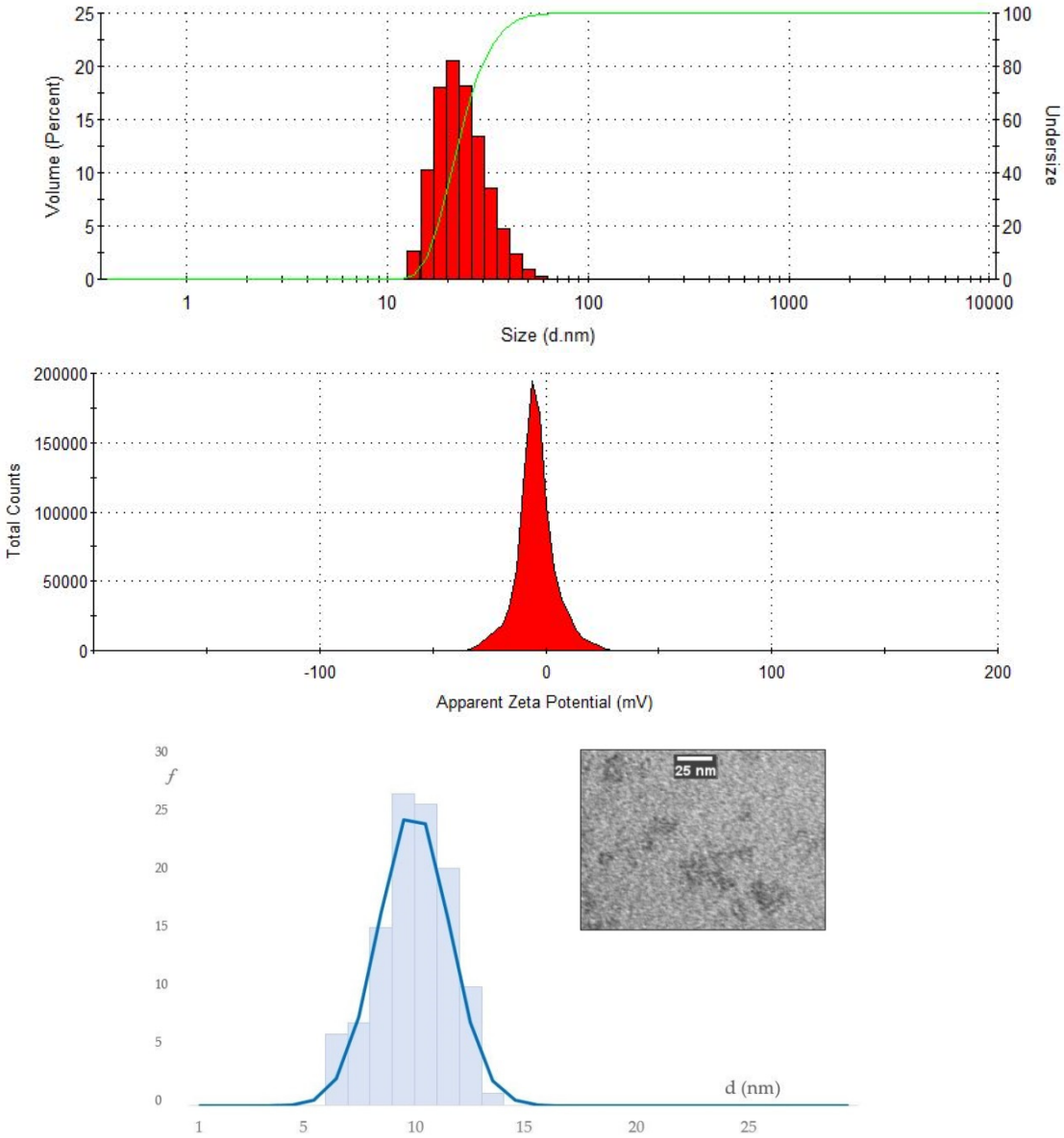

Figure S11. Top, DLS hydrodynamic size distribution by volume of NPs-10%peptide^0; middle, Zeta Potential distribution of NPs-10%peptide^0; bottom, TEM size distribution with representative image of NPs-10%peptide^0 (scale bar 25 nm).

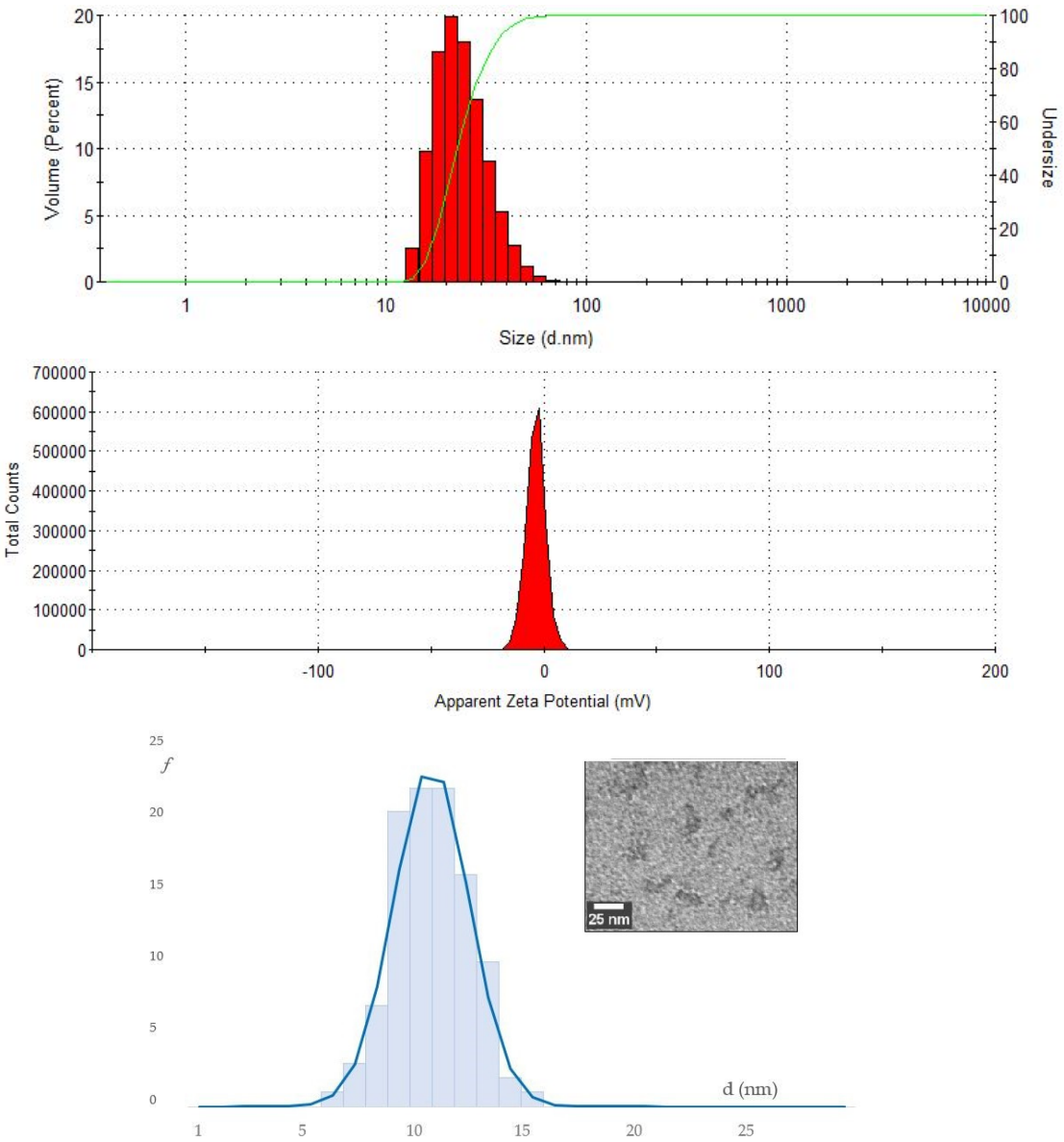

Figure S12. Top, DLS hydrodynamic size distribution by volume of NPs-20%peptide^0; middle, Zeta Potential distribution of NPs-20%peptide^0; bottom, TEM size distribution with representative image of NPs-20%peptide^0 (scale bar 25 nm).

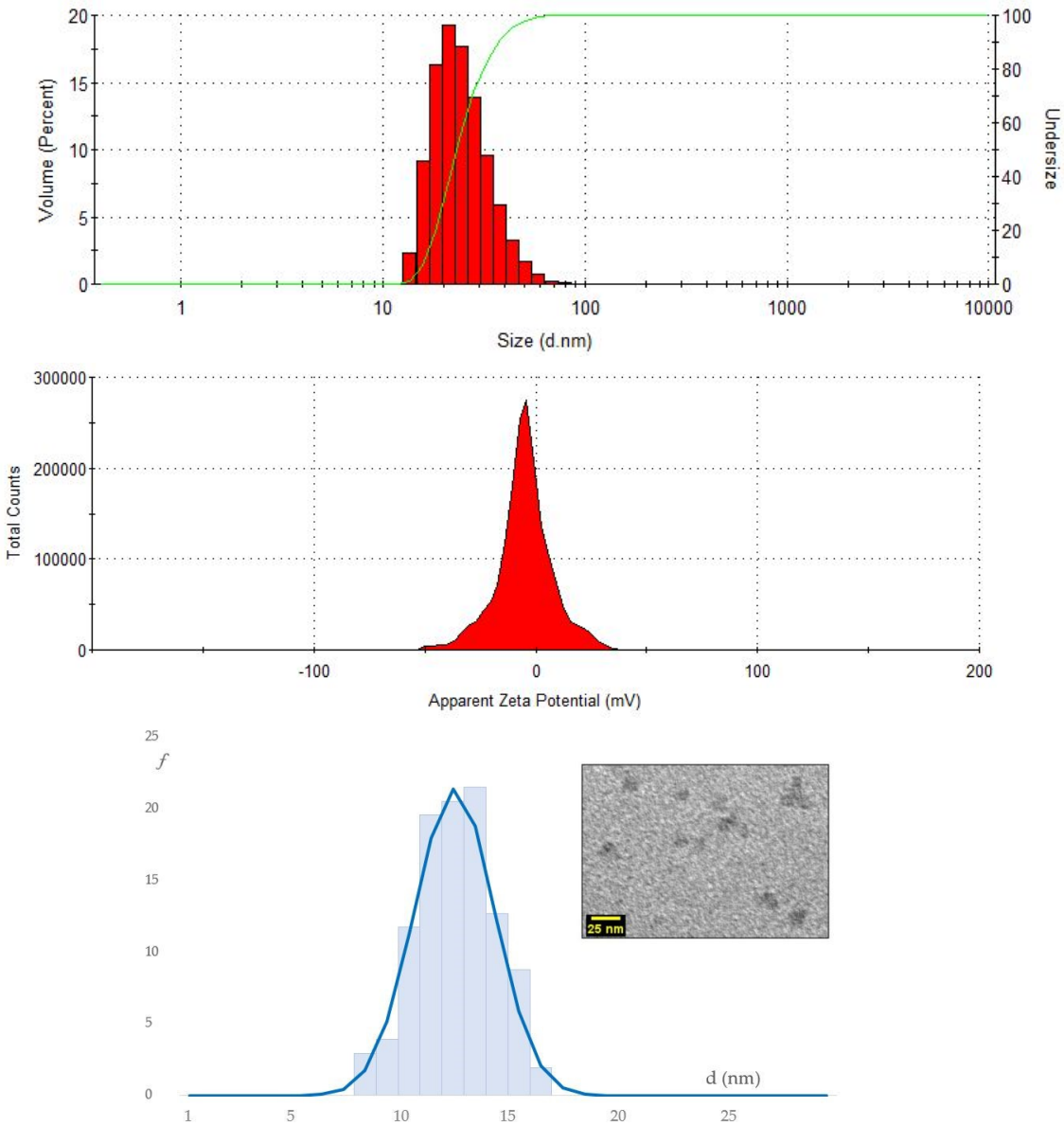

Figure S13. Top, DLS hydrodynamic size distribution by volume of NPs-30%peptide^0; middle, Zeta Potential distribution of NPs-30%peptide^0; bottom, TEM size distribution with representative image of NPs-30%peptide^0 (scale bar 25 nm).

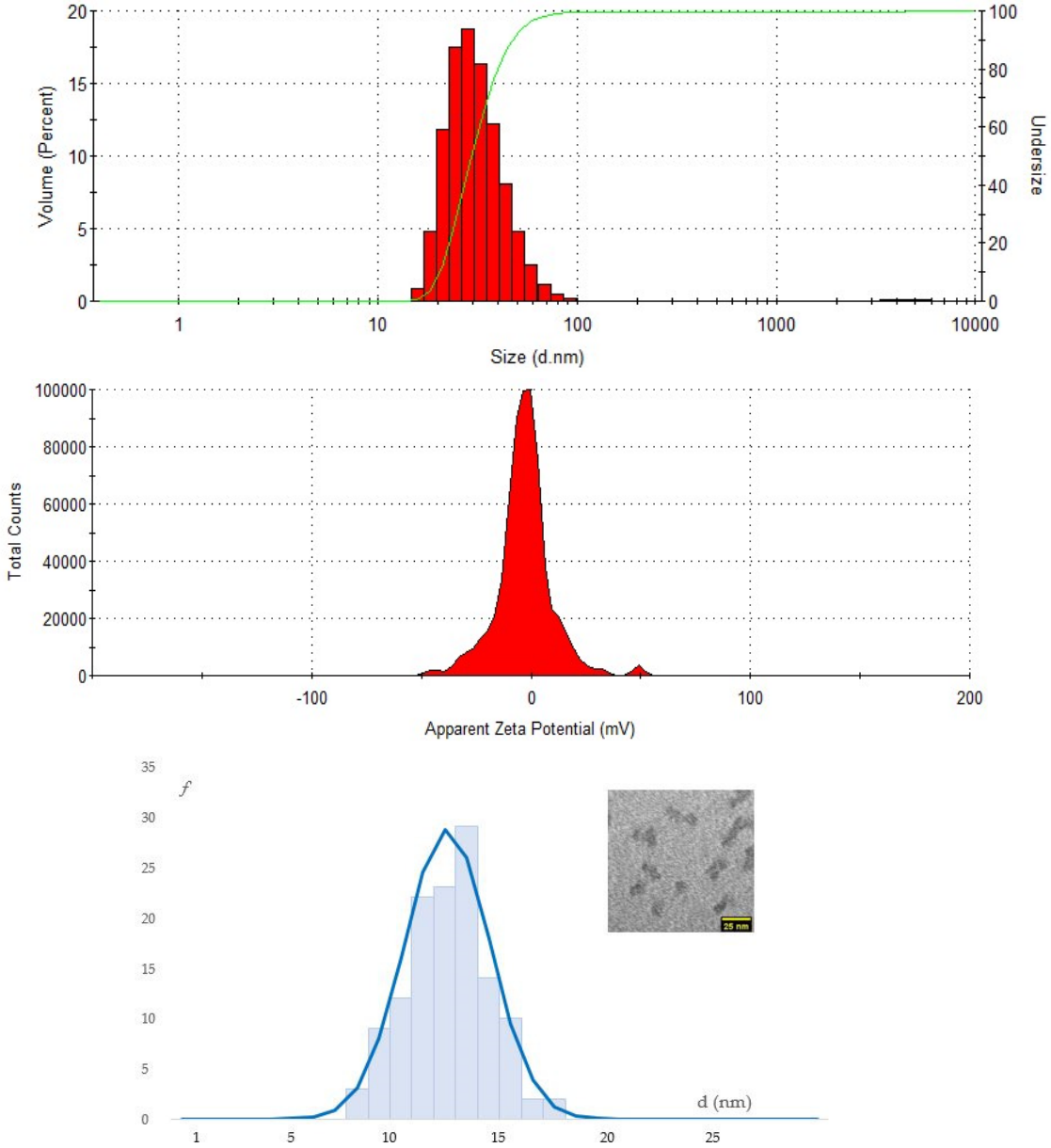

Figure S14. Top, DLS hydrodynamic size distribution by volume of blend NPs-30% peptide; middle, Zeta Potential distribution of blend NPs-30% peptide; bottom, TEM size distribution with representative image of blend NPs-30% peptide (scale bar 25 nm).

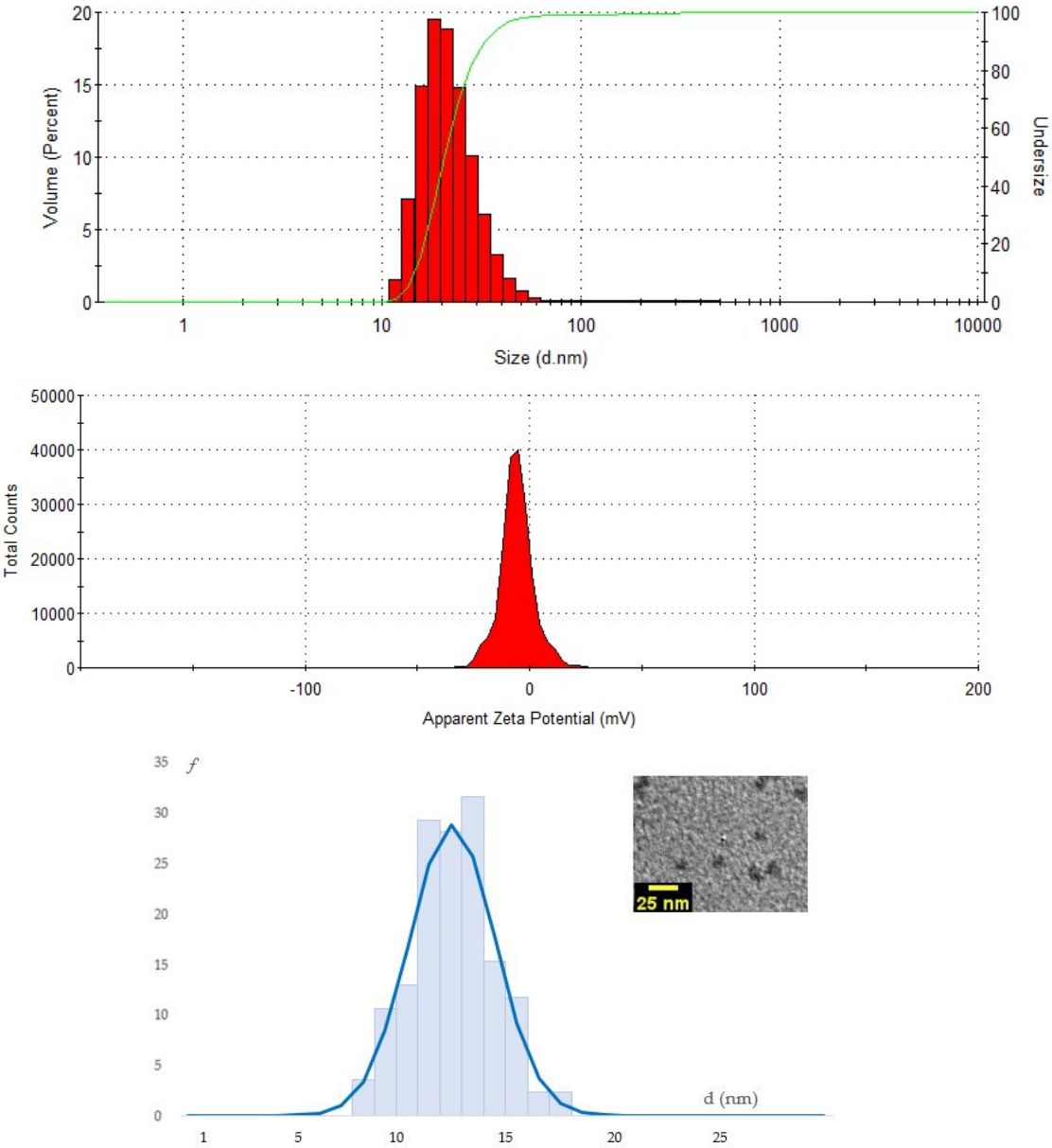

Figure S15. Top, DLS hydrodynamic size distribution by volume of mixed NPs-30% peptide; middle, Zeta Potential distribution of mixed NPs-30% peptide; bottom, TEM size distribution with representative image of mixed NPs-30% peptide (scale bar 25 nm).